Water Induced Chromogenic and Fluorogenic Signal Modulation in a Bi-Fluorophore Appended Acyclic Amino-Receptor System

Bamaprasad Bag* and Ajoy Pal

Colloids and material Chemistry Department,
Institute of Minerals and Materials Technology (CSIR),
Bhubaneswar-751013 India
Email: bpbag@immt.res.in

Supplementary data

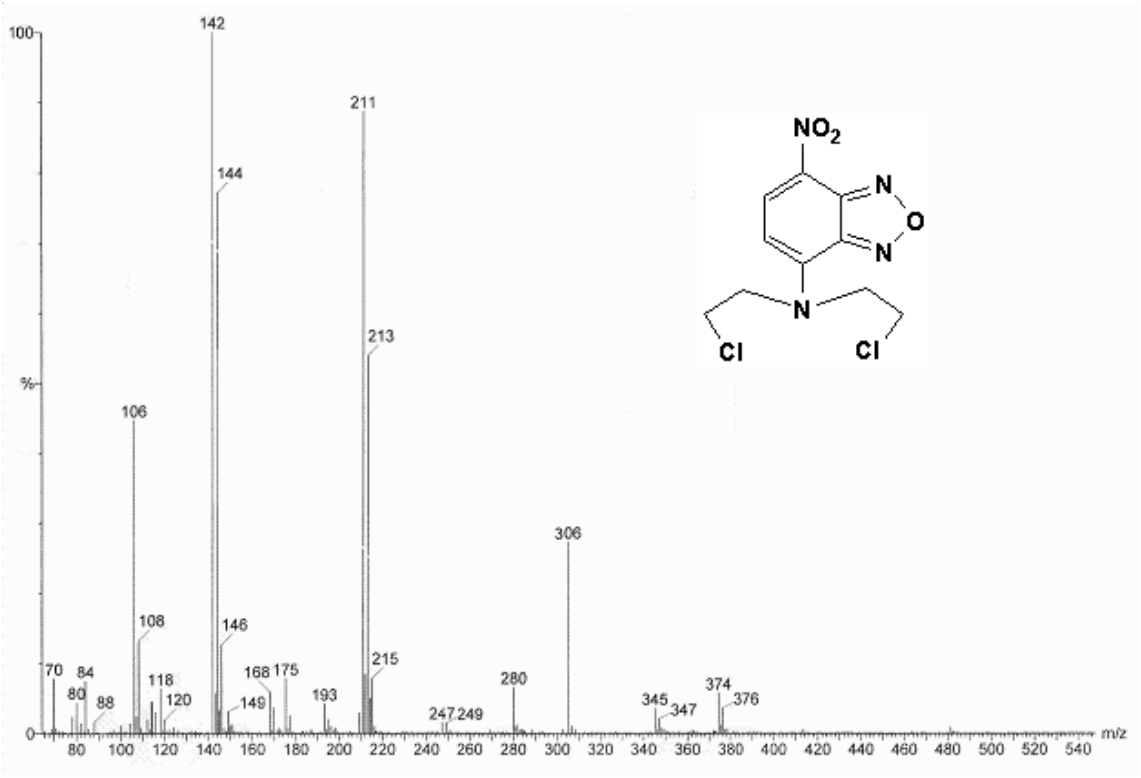

Figure S1. ESI-MS spectrum of **1** [306 = M+1 $(m/z)^+$]

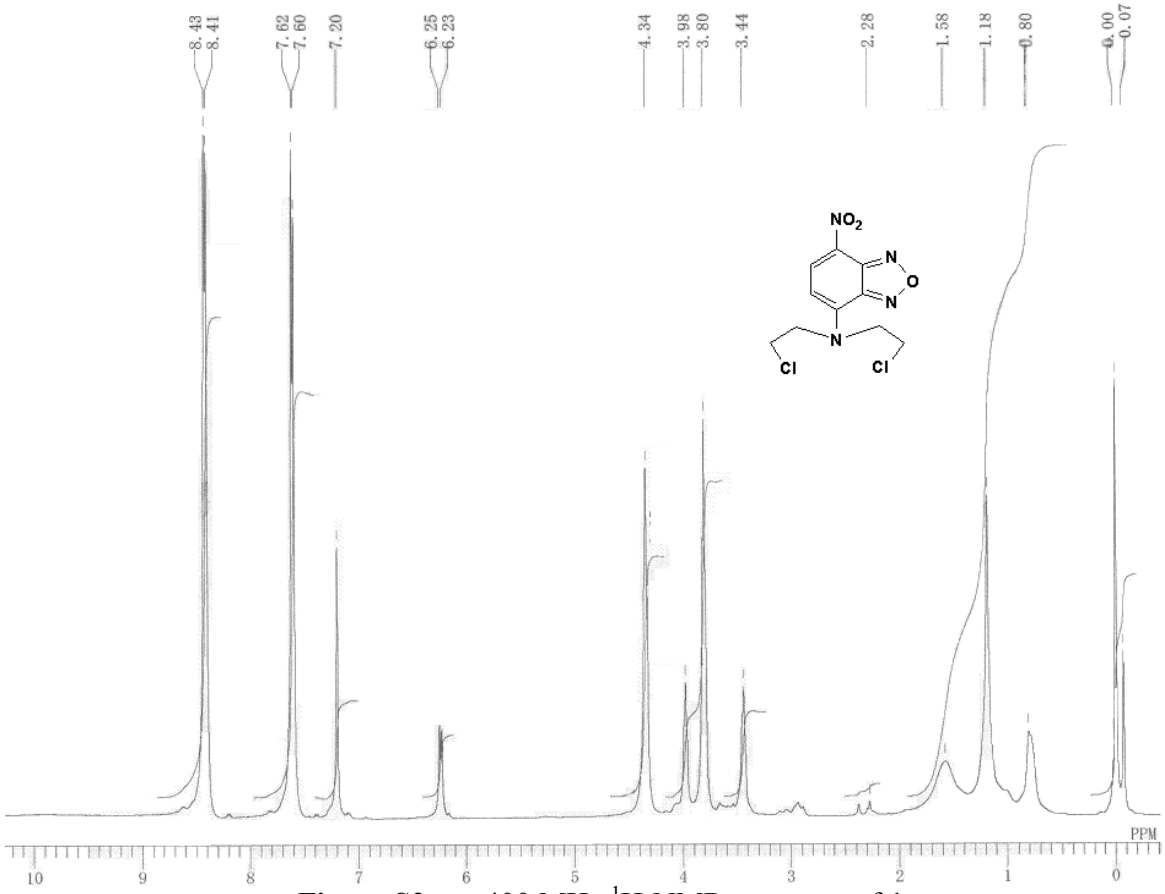

Figure S2. 400 MHz ^{1}H-NMR spectrum of **1**

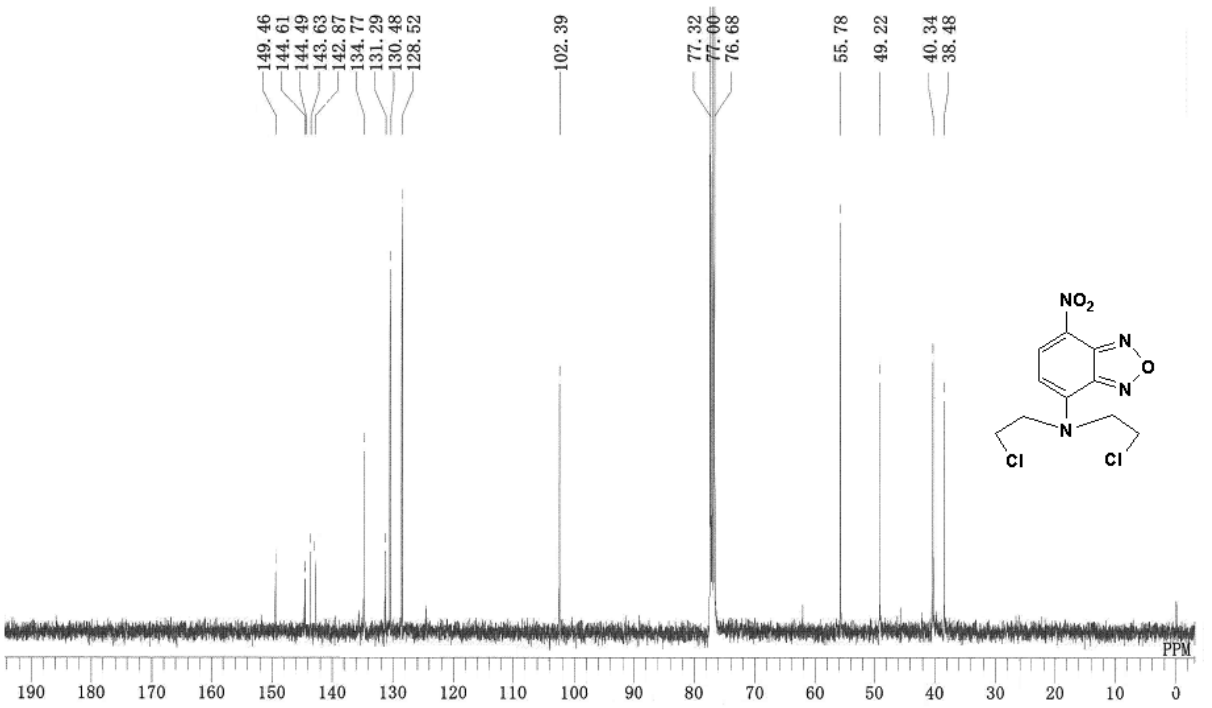

Figure S3 100 MHz ^{13}C-NMR spectrum of **1**

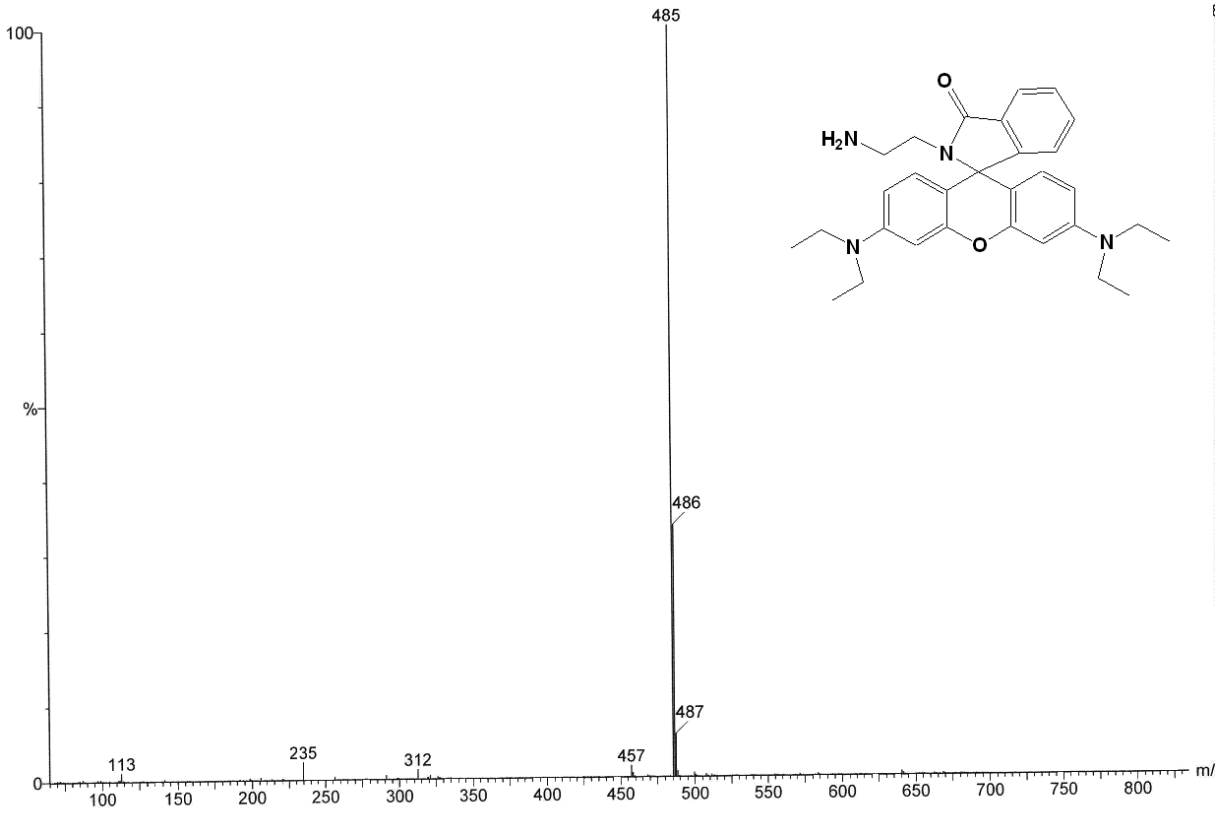

Figure S4: ESI-MS spectrum of **2** [485 = M+1 $(m/z)^+$]

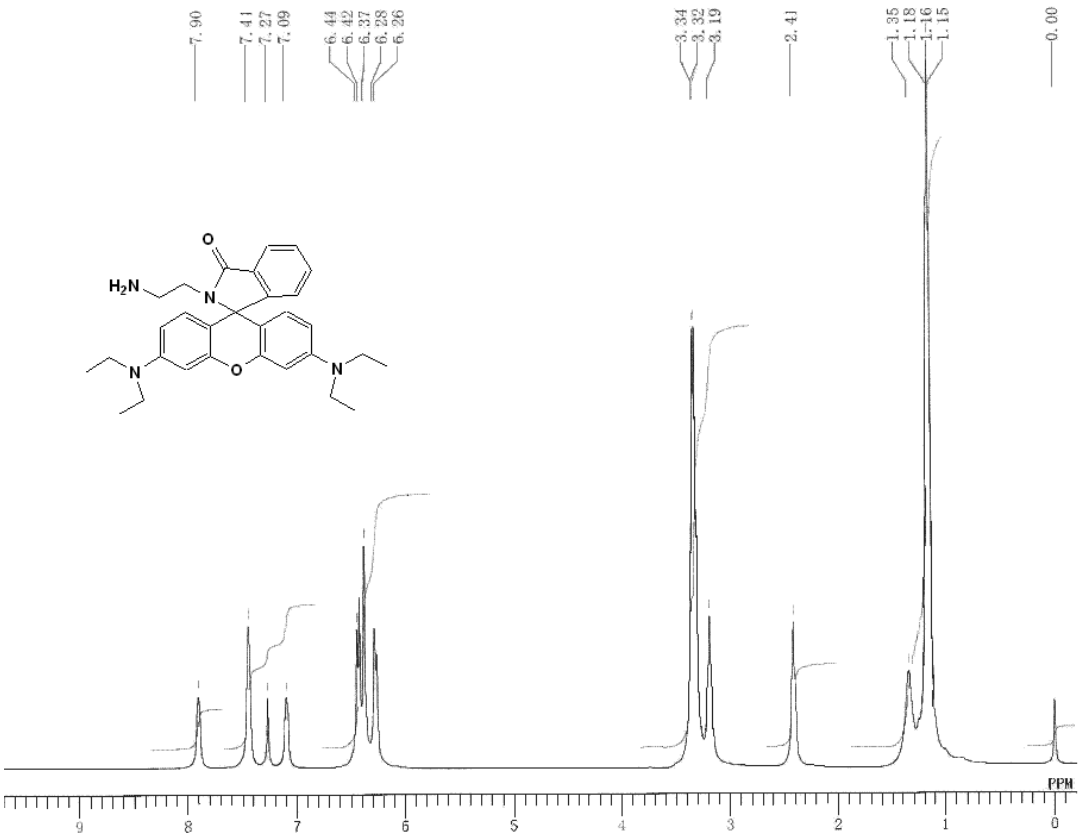

Figure S5. 400 MHz ^{1}H-NMR spectrum of **2**

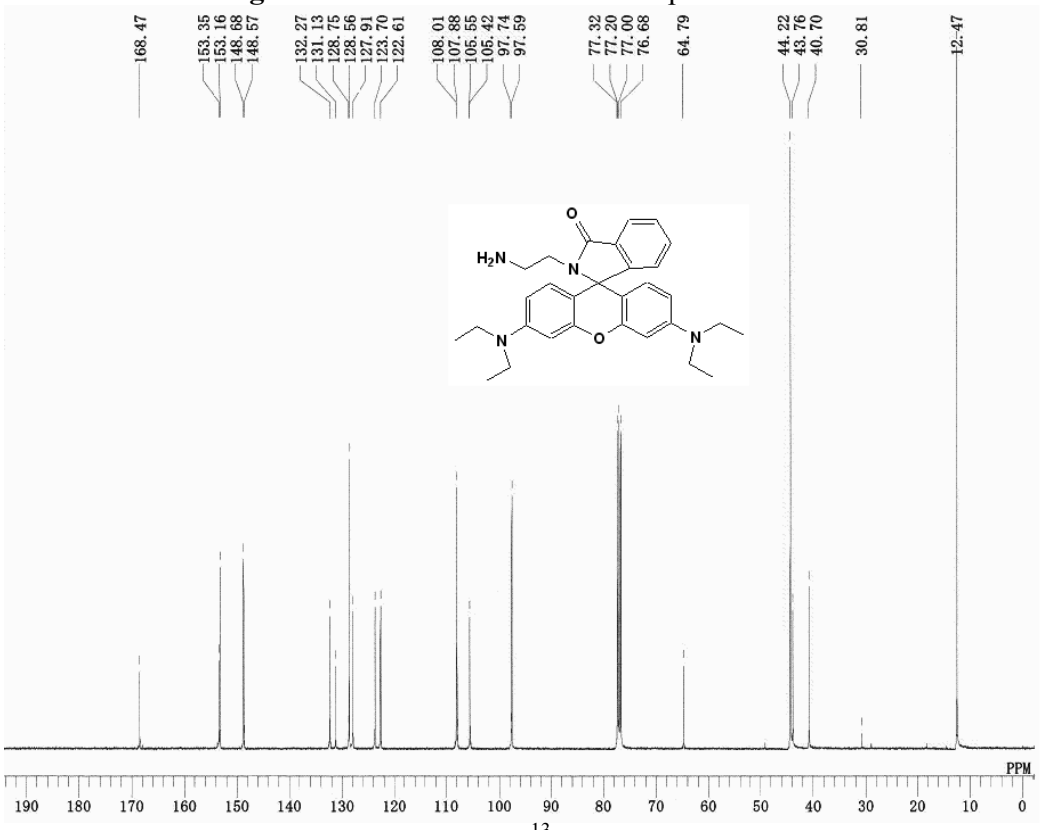

Figure S6. 100 MHz ^{13}C-NMR spectrum of **2**

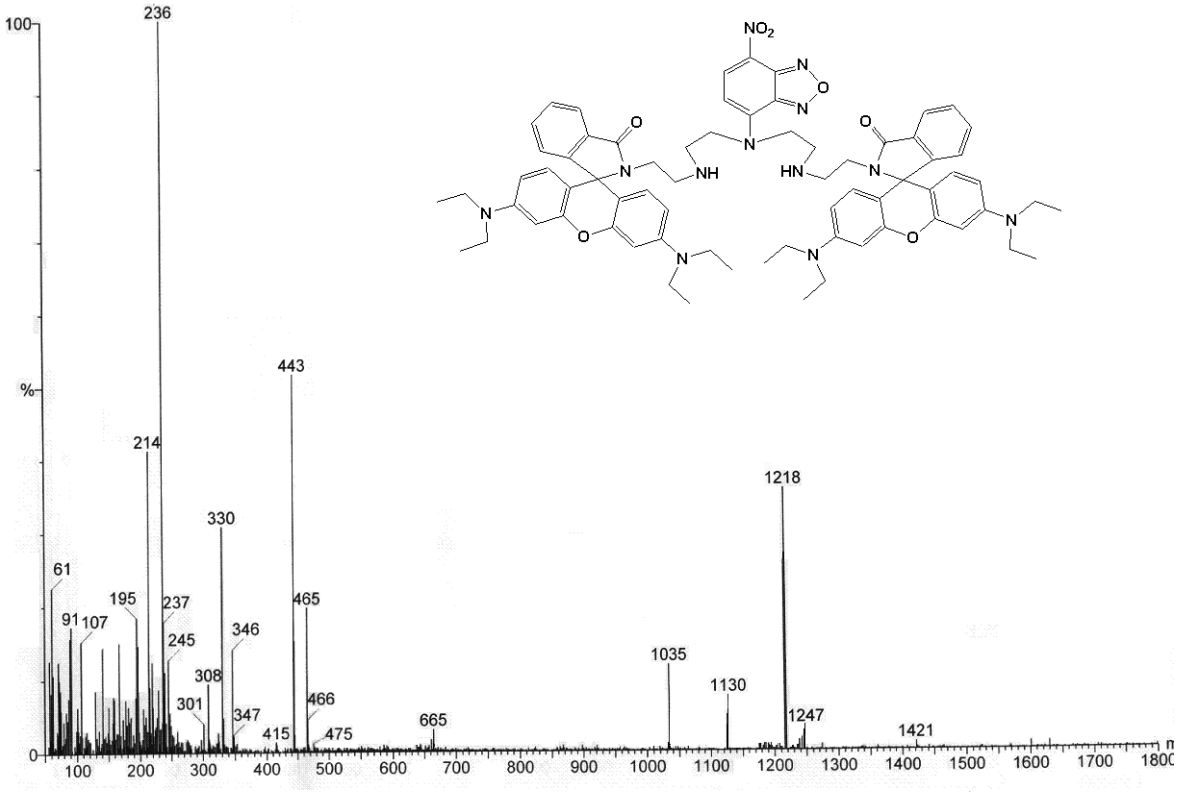

Figure S7: ESI-MS spectrum of **3** [1218 = M.H_2O $(m/z)^+$].

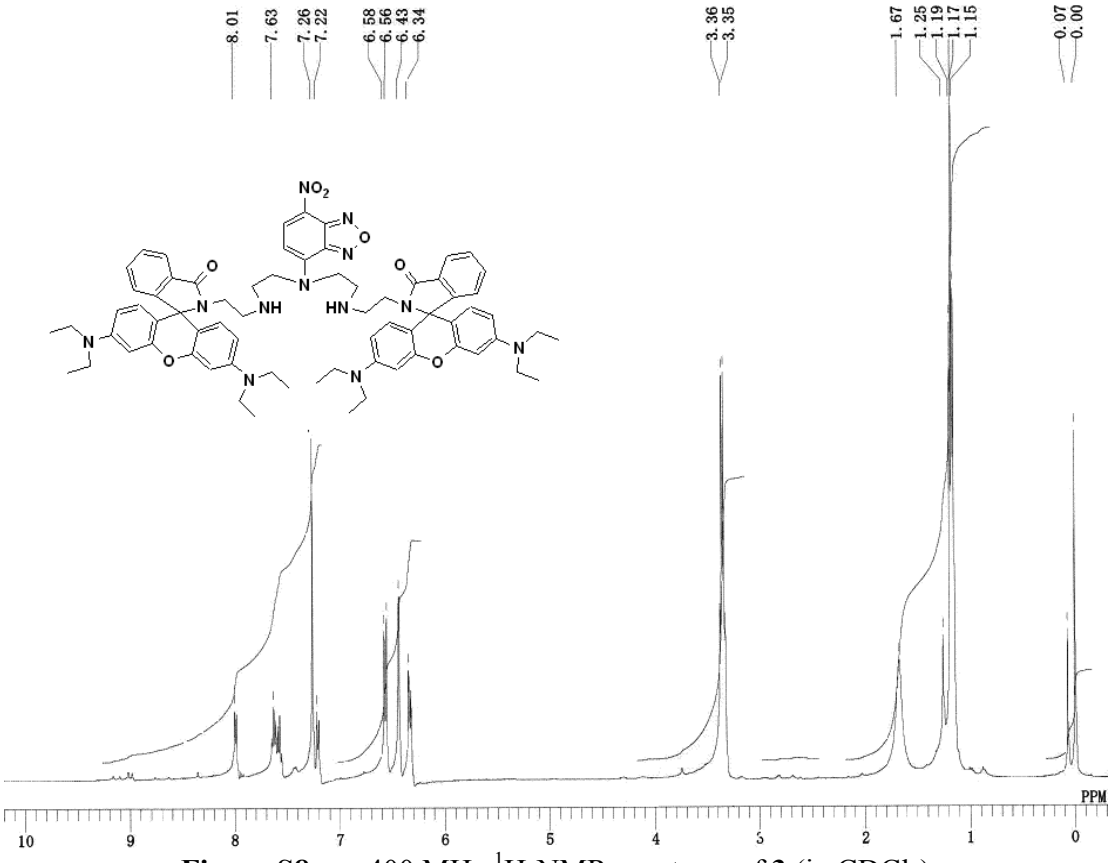

Figure S8. 400 MHz ^{1}H-NMR spectrum of **3** (in $CDCl_3$)

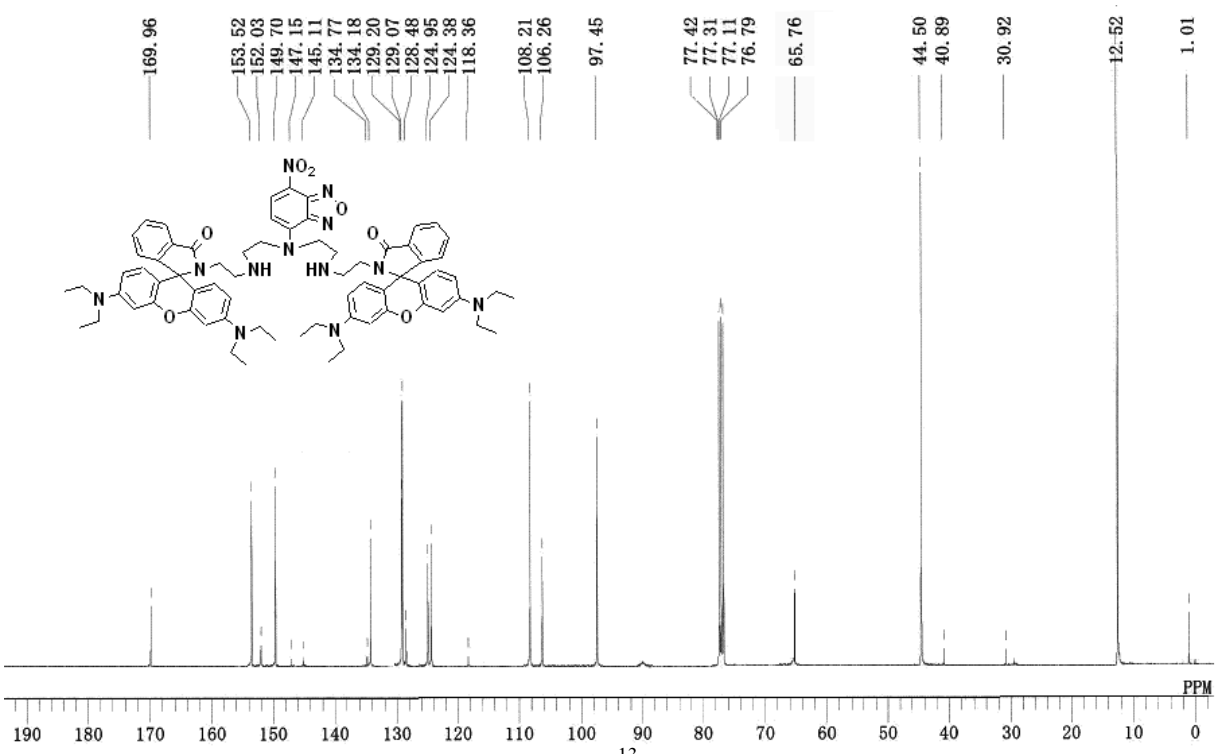

Figure S9. 100 MHz ^{13}C-NMR spectrum of **3**

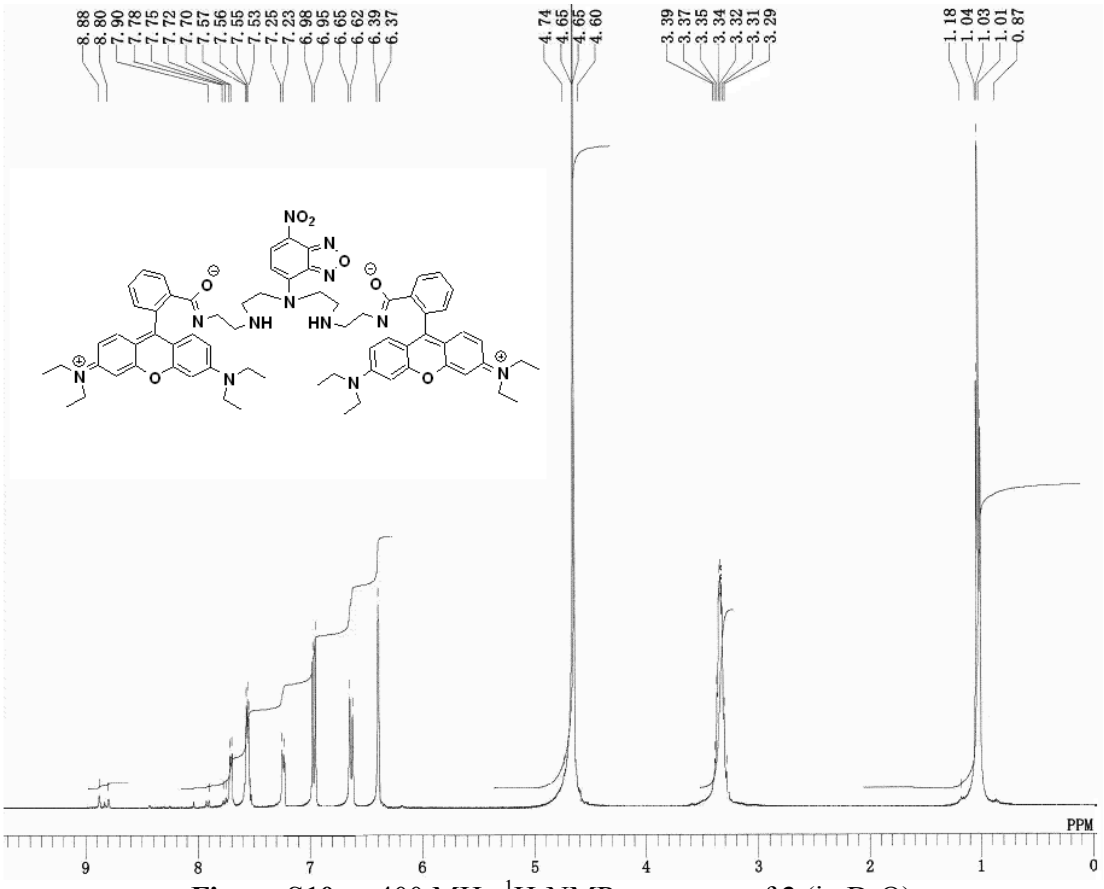

Figure S10. 400 MHz ^{1}H-NMR spectrum of **3** (in D_2O)

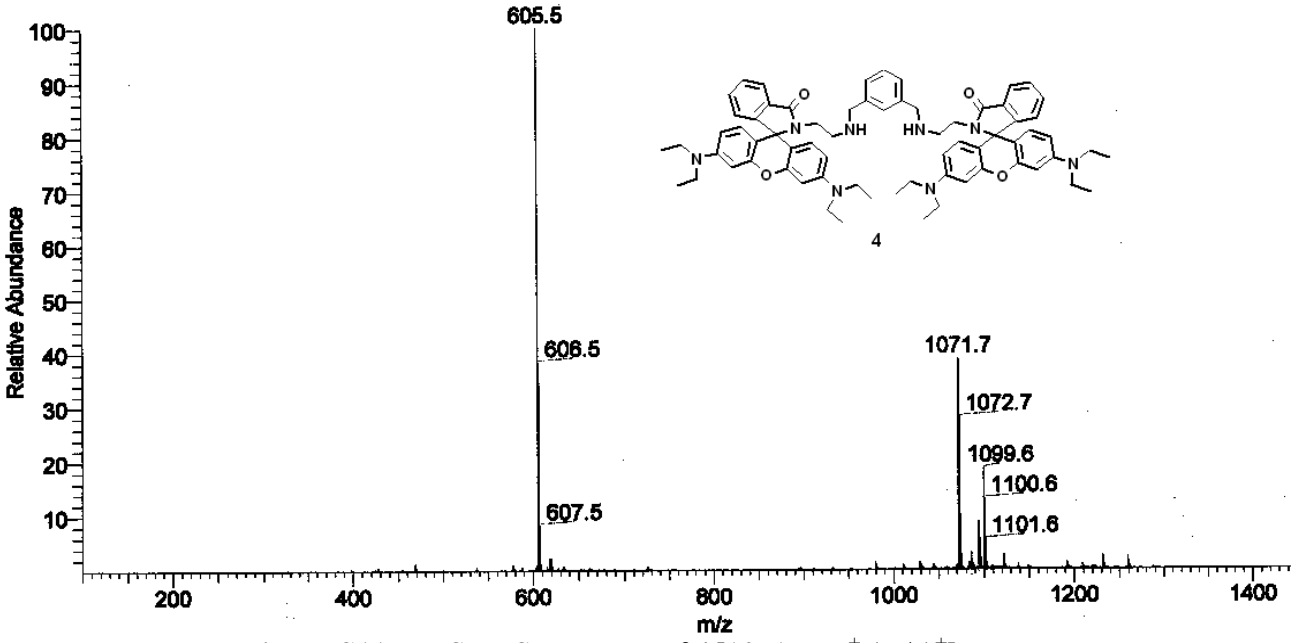

Figure S11. ESI-MS spectrum of **4** [1071 = M^+ $(m/z)^+$].

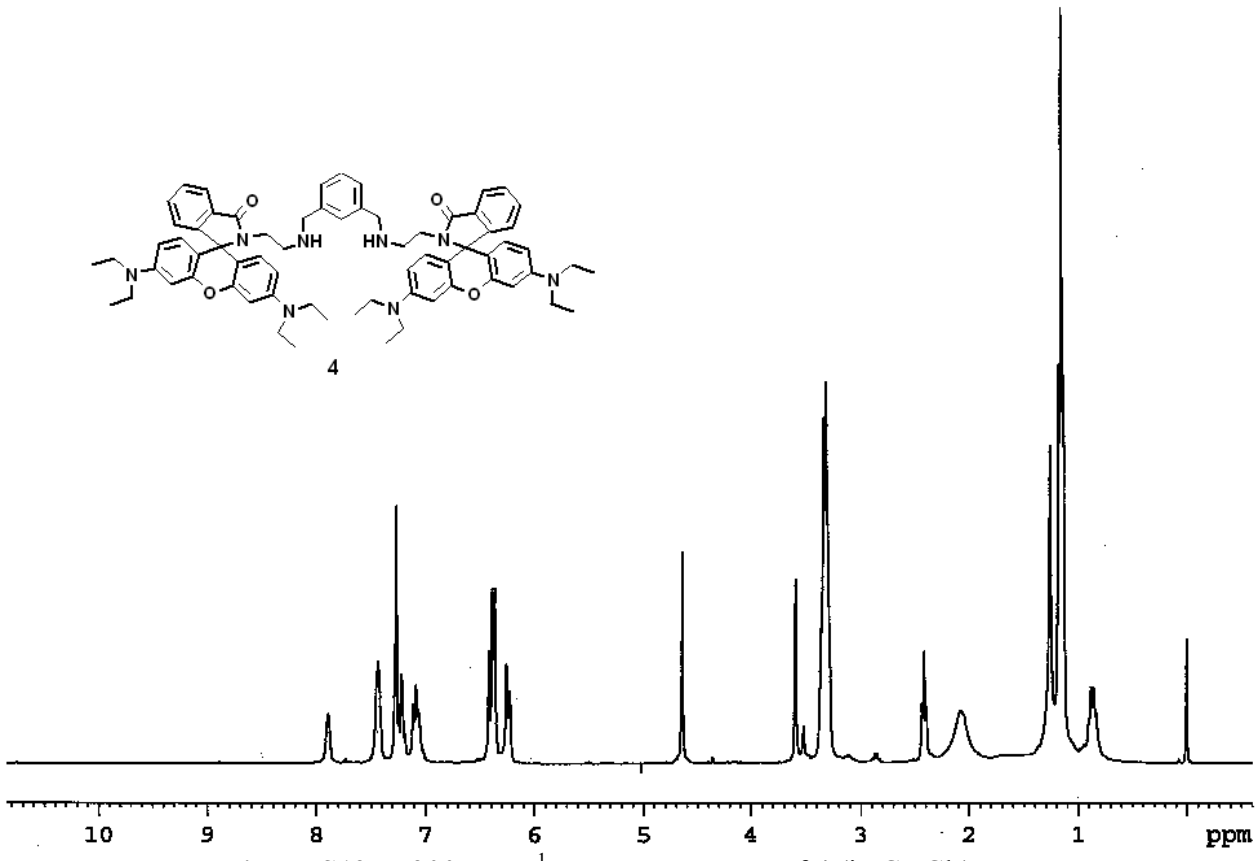

Figure S12. 300 MHz ^{1}H-NMR spectrum of **4** (in $CDCl_3$)

Table S1 Absorption peak position (λ, nm) and corresponding molar extinction coefficient (ε, $dm^3mol^{-1}cm^{-1}$) of **1-3** in different solvents (conc.1×10^{-6} M)

Ligand	Solvent	λ,nm (ε, $dm^3\ mol^{-1}\ cm^{-1}$)		
1	n-Hexane	434 (s, n. d.)	331 (n. d.)	268 (n. d.)
	$CHCl_3$	456 (31732),	333 (36521),	265 (14167)
	Ethyl Acetate	457 (10641),	320 (11367),	269 (15039)
	THF	461 (4135),	322 (3838),	
	DCM	458 (24577),	337 (36673),	264 (16778)
	DMSO	475 (14907),	336 (18019),	259 (7470)
	DMF	473 (14472),	347 (6702),	271 (9340)
	Acetone	464 (15312)	-	
	Ethanol	463 (5273),	333 (5845),	264 (2708)
	Acetonitrile	468(5848),	337 (4588),	276 (3060, s)
	Methanol	464 (12249),	334 (15281)	265 (8915, s)
2	n-Hexane	500 (n. d.),	308 (n. d.),	270 (n. d.)
	$CHCl_3$	495 (23),	316 (78015),	274 (197360)
	Ethyl Acetate	495 (23),	311 (57947),	272 (183184)
	THF	504 (16),	312 (28858),	273 (65393)
	DCM	500 (25),	316 (49733),	275 (143000)
	DMSO	499 (20),	315 (45545),	271 (111957)
	DMF	498 (17),	315 (45520),	272 (111538)
	Acetone	502 (20)		
	Ethanol	504 (28),	312 (30957) ,	272 (85231)
	Acetonitrile	496 (20),	314 (35172),	273 (95524)
	Methanol	508 (42),	313 (63587),	274 (172849)
3	n-Hexane	557 (n. d.), 415 (n. d.), 307 (n. d.), 271 (n. d.)		
	1,4-Dioxane	561 (1435), 383 (5575)		
	$CHCl_3$	554 (23626), 315 (94685), 276 (161603)		
	Ethyl Acetate	556 (643), 312 (40503), 273 (86213)		
	THF	556 (992), 395 (2660), 312 (99790), 274 (178759)		
	DCM	558 (22796), 315 (104597), 278 (177569)		
	DMSO	560 (992), 401 (2043), 315 (49149), 275 (92875)		
	DMF	560 (938), 402 (2231), 316 (49090), 275 (93924)		
	Acetone	559 (5755), 395 (9227)		
	Ethanol	542 (325269), 502 (92716), 393 (18154), 355 (33712), 304 (56017), 257 (112086)		
	Acetonitrile	552 (1795), 317 (87867), 275 (165880)		
	Methanol	544 (345787), 400 (17086), 353 (39993), 305 (62634), 279 (69569)		

Table S2 Emission maxima and fluorescence quantum yield (ϕ_F) of **1-3** in different solvents[a].

Ligand	Solvents	λ^{em}_{max} (nm)	Quantum Yield (ϕ_F)
1	n-Hexane	494	n. d.
	$CHCl_3$	514	0.041
	Ethyl Acetate	519	0.007
	THF	526	0.001
	DCM	525	0.037
	DMSO	530	0.001
	DMF	532	0.001
	Acetone	530	0.001
	Ethanol	527	0.002
	Acetonitrile	530	0.001
	Methanol	532	0.002
2	n-Hexane	517	n. d.
	$CHCl_3$	536	0.009
	Ethyl Acetate	530	0.019
	THF	536	0.017
	DCM	534	0.025
	DMSO	536	0.004
	DMF	534	0.003
	Acetone	534	0.002
	Ethanol	539	0.013
	Acetonitrile	530	0.007
	Methanol	538	0.009
3	n-Hexane	562	n. d.
	$CHCl_3$	564	0.249
	Ethyl Acetate	567	0.035
	THF	568	0.009
	DCM	566	0.355
	DMSO	588	0.002
	DMF	587	0.002
	Acetone	579	0.013
	Ethanol	630	0.291
	Acetonitrile	575	0.005
	Methanol	629	0.256

[a]Experimental Conditions: Concentration of free ligands: 1×10^{-6} M; $\lambda_{ex} = \lambda_{abs}$(400-600 nm, varies with solvent); excitation and emission band-pass: 5 nm; T= 298 K; ϕ_F was calculated by comparison of corrected spectrum with that of Rhodamine G ($\phi_F = 0.95$) in EtOH taking the area under the total emission. The error in ϕ_F is within 15 %.

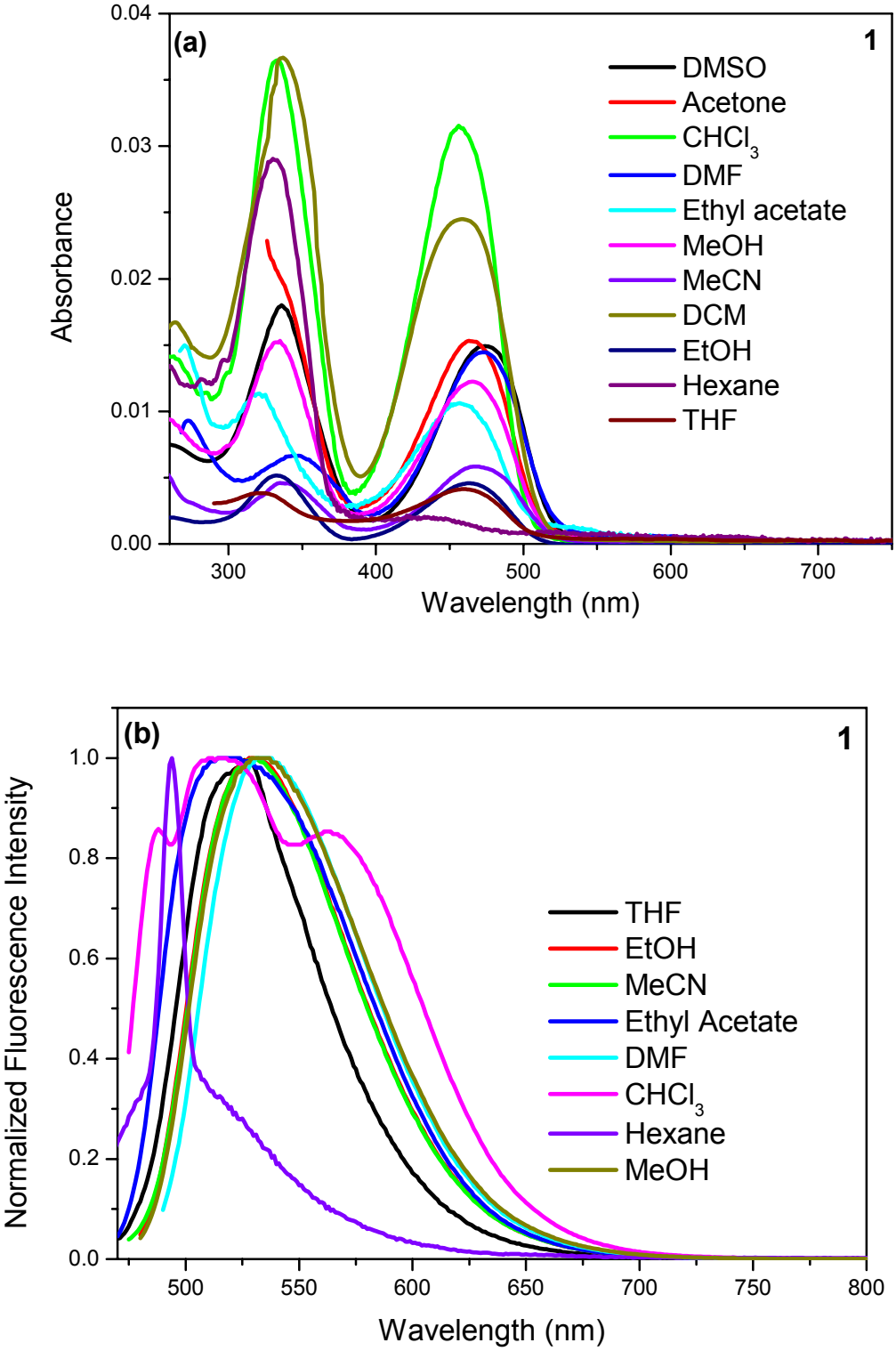

Figure S13. Absorption (a) & normalized emission (b) spectra of **1** in various solvents. Absorption: concentration =1 × 10^{-6} M; Emission experimental conditions: 1 × 10^{-6} M; λ_{ex} = λ_{abs}(400-600 nm, varies with solvent), emission and excitation band pass: 5 nm, Temperature: 298 K.

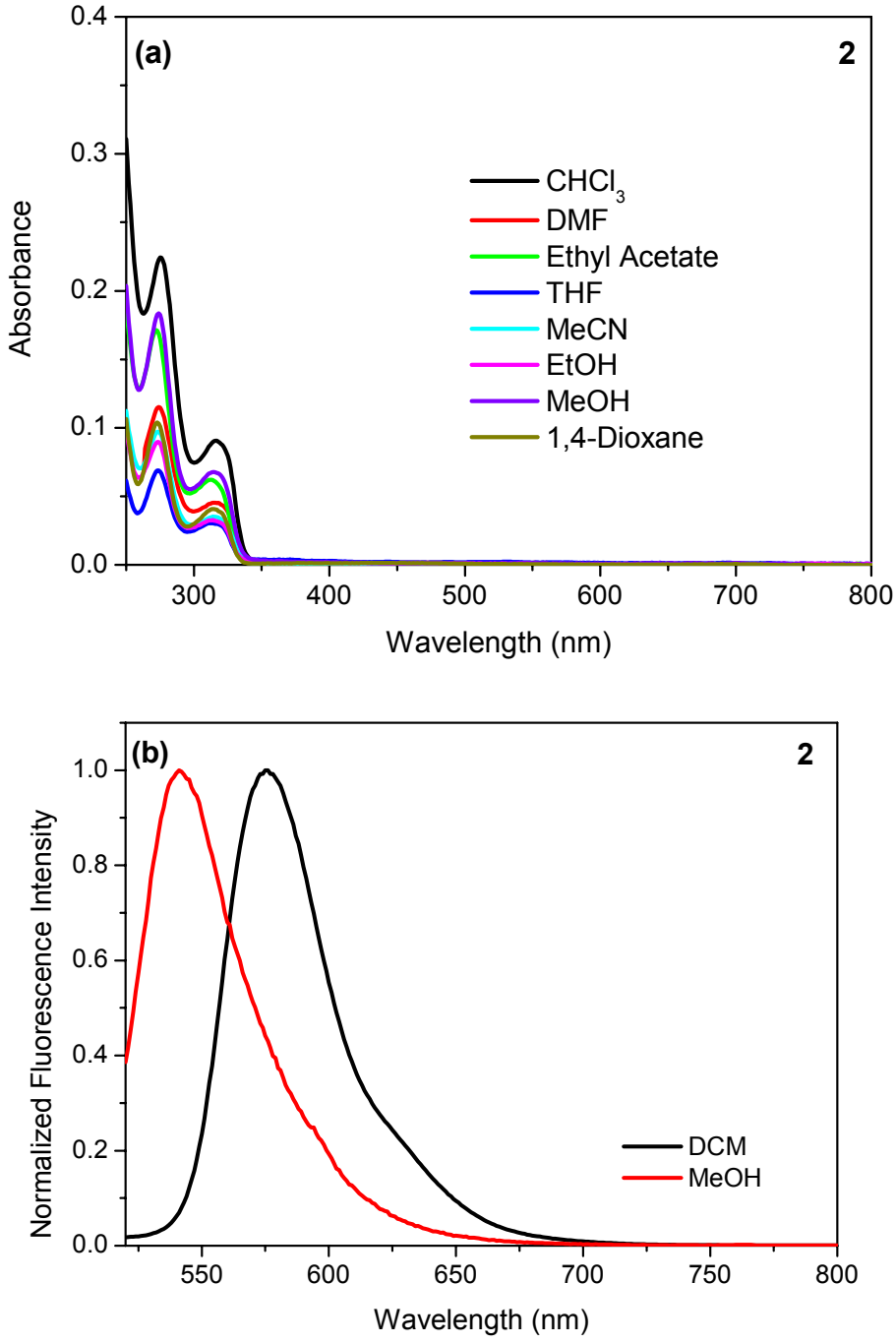

Figure S14 Absorption (a) and Normalized fluorescence (b) spectra of **2** in various solvents. [Conc. = 1×10^{-6} M]. From the emission spectra, it is apparent that the ground state is more stabilized in polar solvents than in non-polar solvents causing blue-shift of emission.

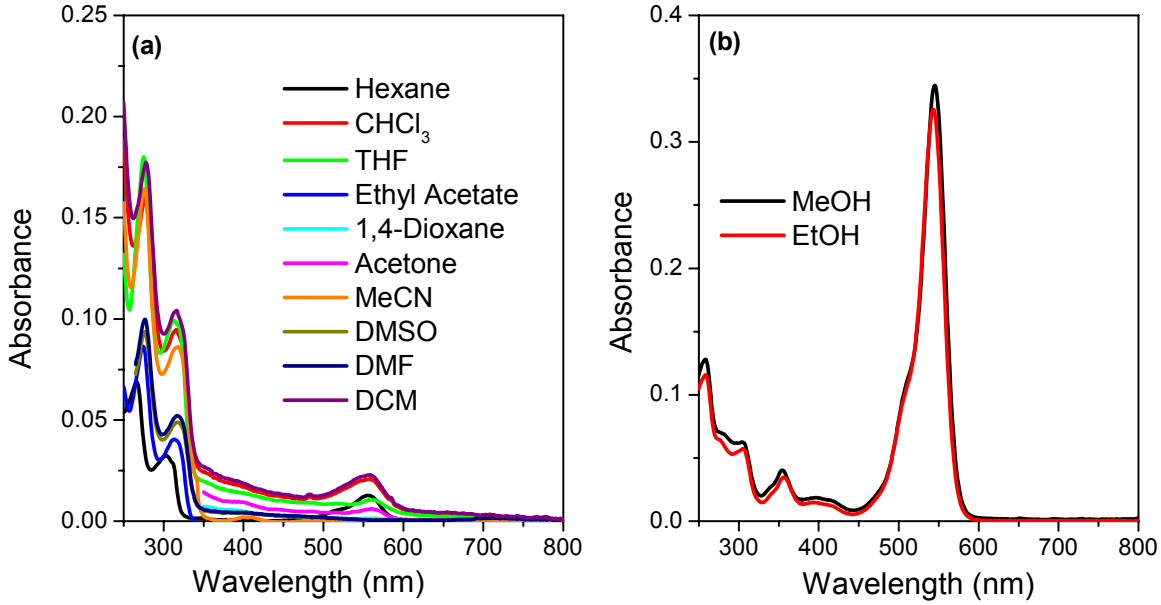

Figure S15. Absorption spectra of **3** in various solvents (conc. 1×10^{-6} M).

From the figure, it is apparent that the solution of **3** in the solvents in (b) exhibits pink colour with a higher molar extinction coefficient (ε) of absorption at ~550 nm whereas the colorless solution in solvents in (a) do not absorb or fairly absorb in that region. The little absorption with a lower molar extinction coefficient in 500-600nm region in the solvents in Fig S15-(a) may be due to trace of ring-opened molecules of **3** [Ref: Y. Xiang, and A. Tong, *Org. Lett*. 2006, **8**, 1549]. The absorption with a high molar extinction coefficient in 500-600 nm region in the solvents in Fig S15-(b) may be attributed to the solvent assisted ring opening of the *spiro*-form of rhodamine in **3**. The mechanism of solvent-assisted ring opening is yet to be properly understood, however, the function of solvent polarity may be excluded for deducing the mechanism as apparent from these spectroscopic data.

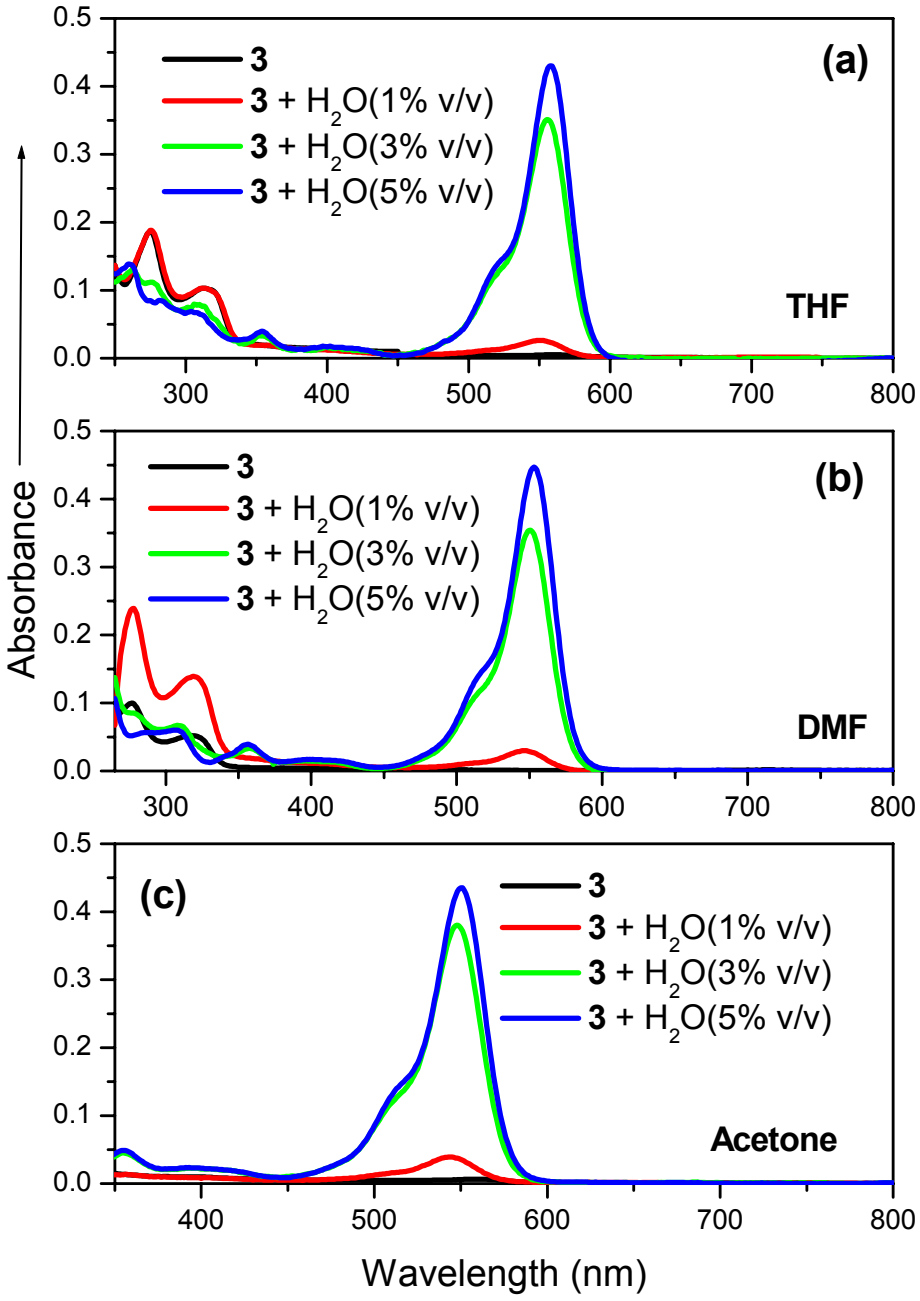

Figure S16. Absorption spectra of **3** in presence of H_2O in (a) THF, (b) DMF and (c) Acetone. [conc. = 1×10^{-6} M].

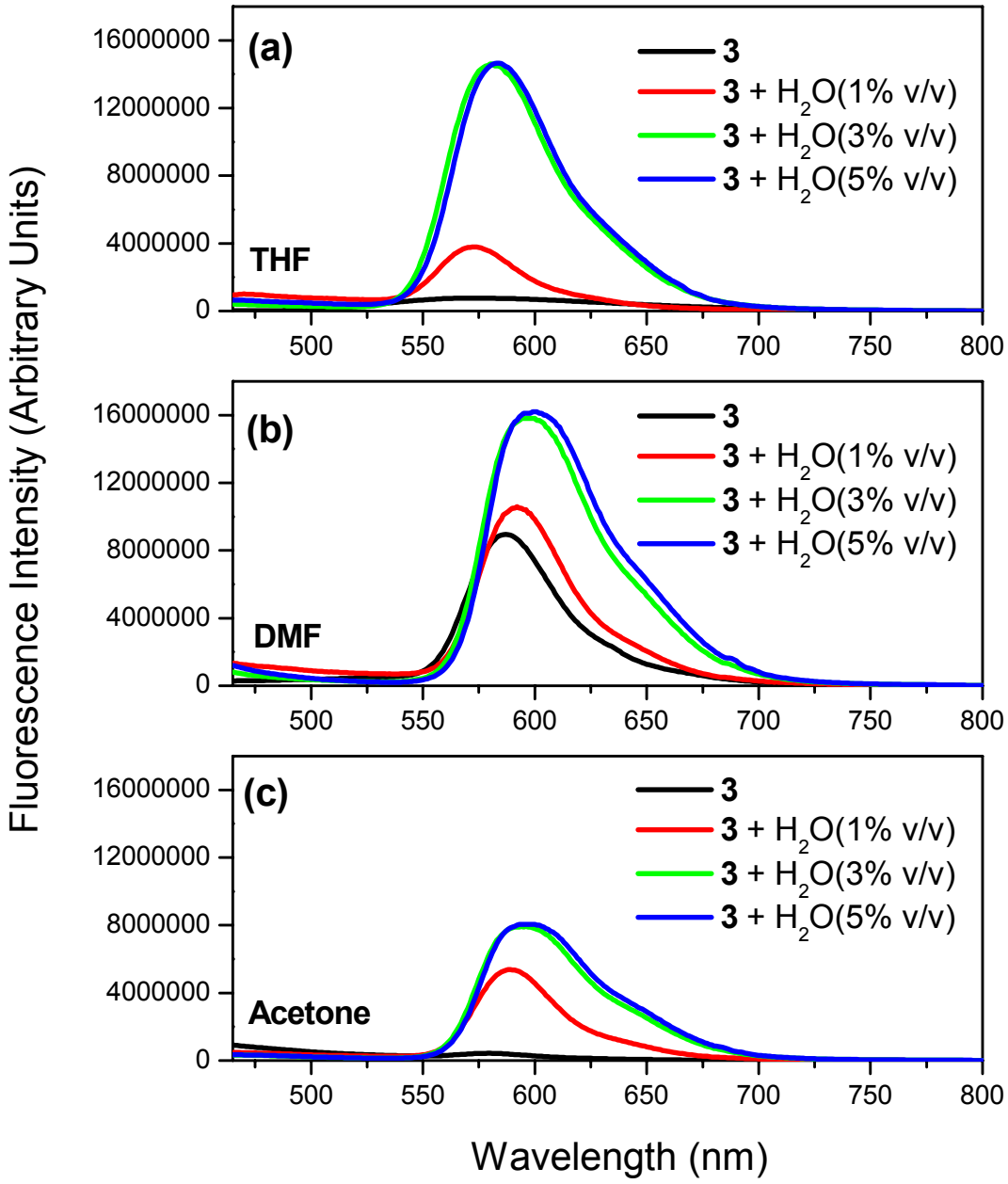

Figure S17. Emission spectra of **3** in presence of H_2O in (a) THF, (b) DMF and (c) Acetone. Concentration of free ligand: 1×10^{-7} M, λ_{ex} = 450 nm.

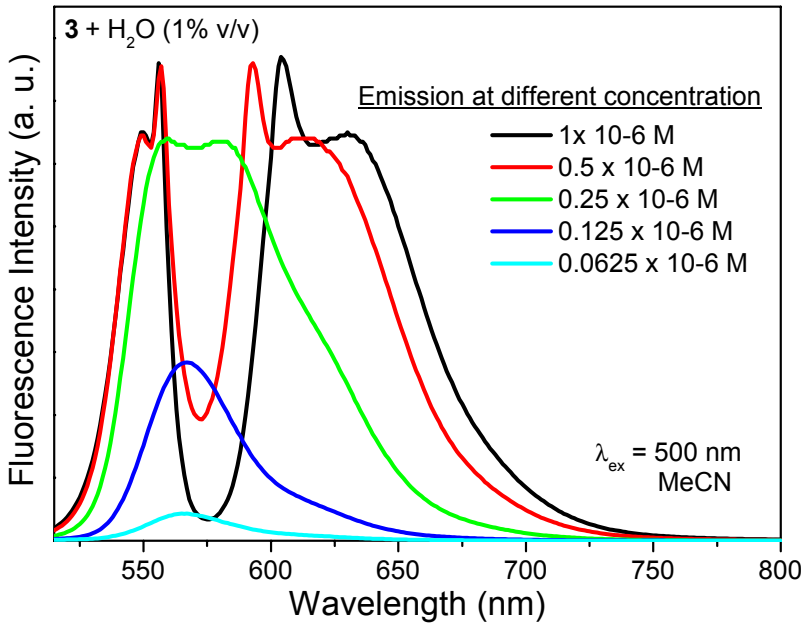

Figure S18. Emission spectra of **3** in presence of H_2O (1% v/v) in MeCN at different concentration excited at 500nm indicating excimer formation at 620nm.

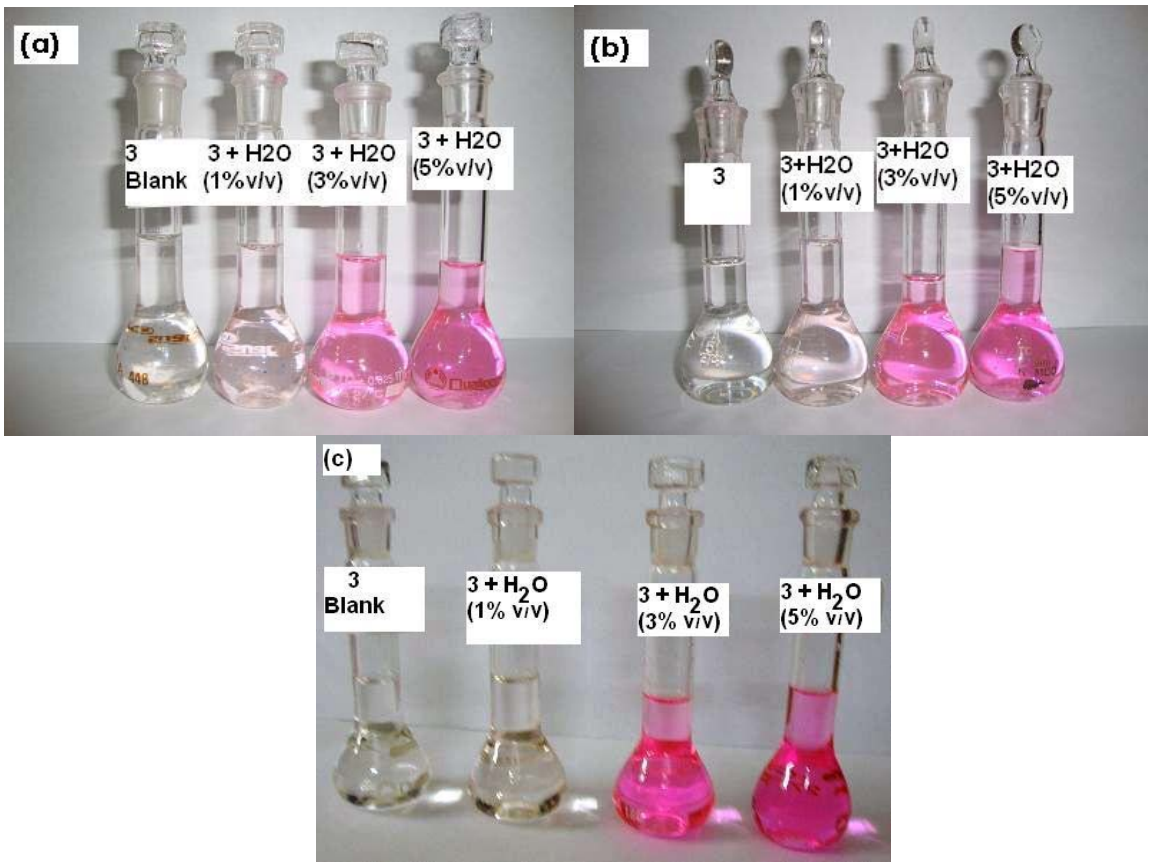

Figure S19. Photographs of **3** alone and in presence of H_2O in different proportions in (a) Acetone, (b) DMF and (c) DMSO. [conc. 1×10^{-6} M]

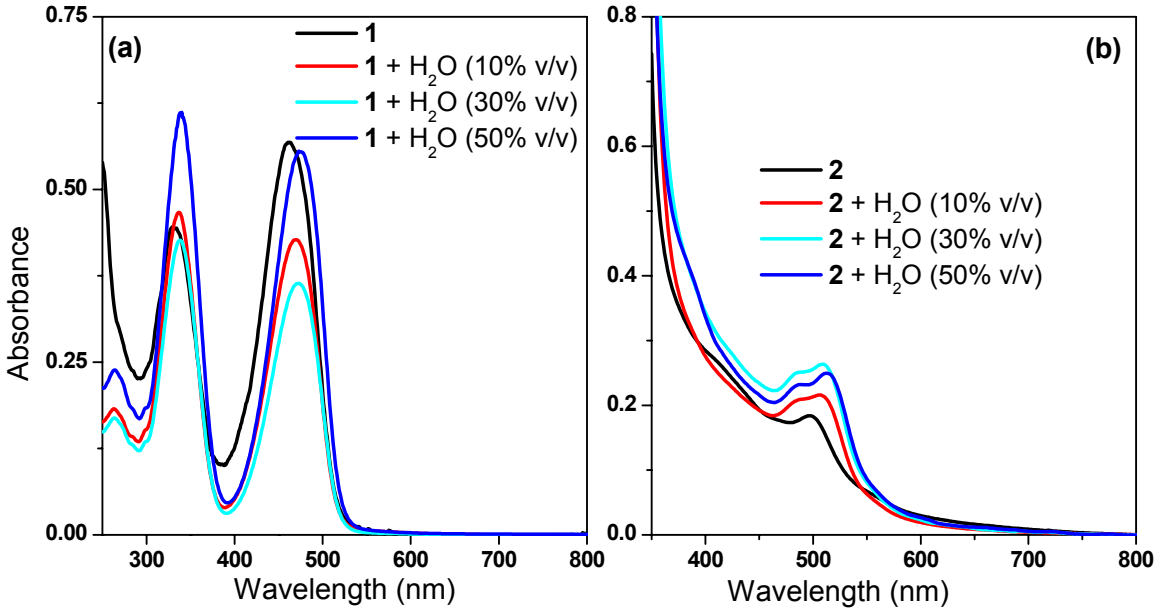

Figure S20. Absorption spectra of (a) **1** and (b) **2** in presence of H_2O in MeCN. Conc. of **1** = 1×10^{-4}M; conc. of **2** = 1×10^{-2}M; added water in % of v/v with MeCN.

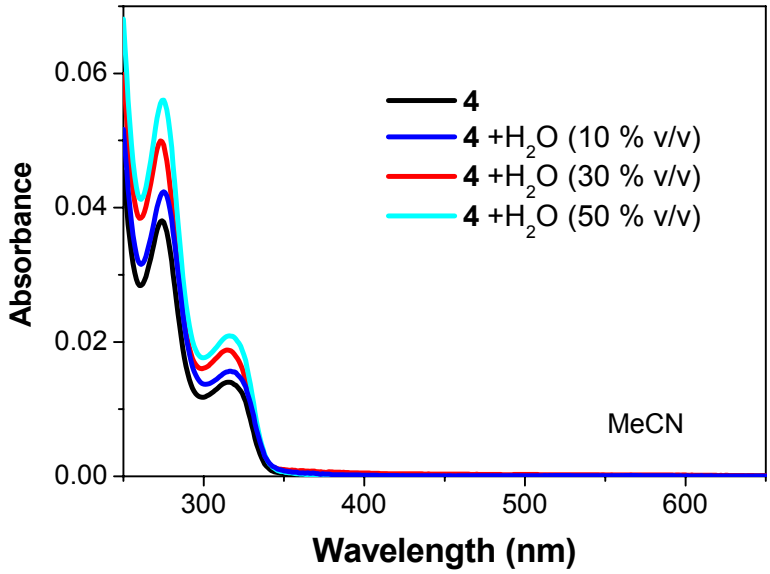

Figure S21. Absorption spectra of **4** in presence of H_2O in MeCN [conc. of **4** = 1×10^{-6}M]

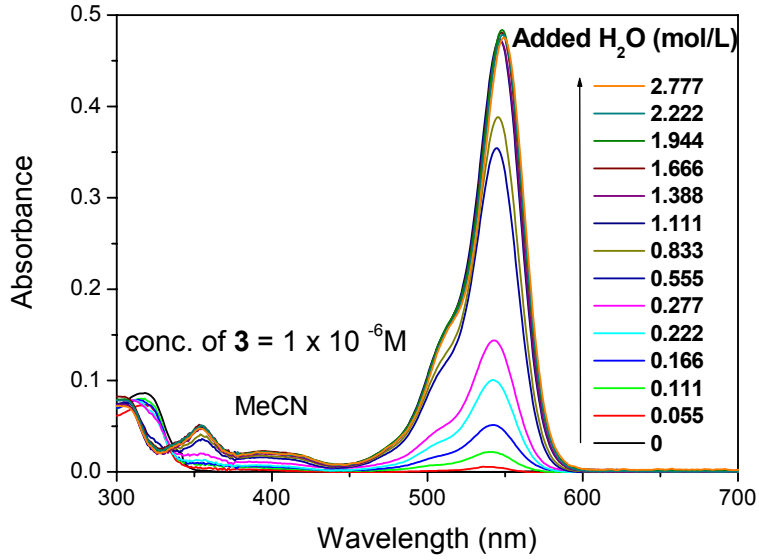

Figure S22. Absorption spectra of **3** as a function of added H_2O [mol/L] in MeCN.

Figure S23. Photograph of **3** as a function of added H_2O (% v/v) in MeCN(conc. 1×10^{-6} M).

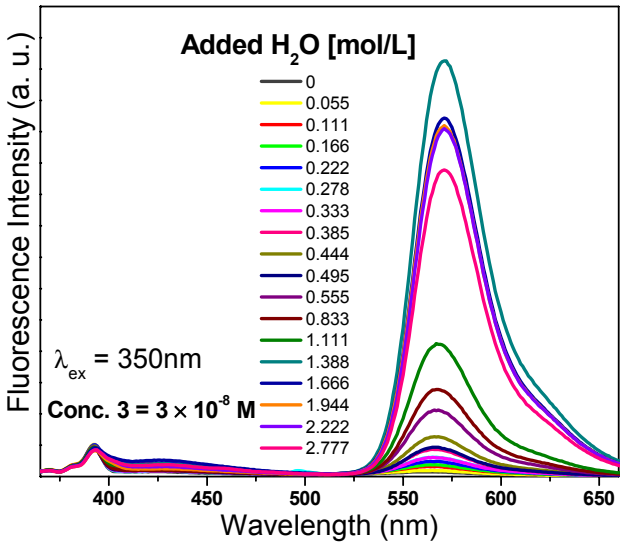

Figure S24. Fluorescence spectra of **3** (MeCN, 1×10^{-8}M) as a function of added H_2O [mol/L].

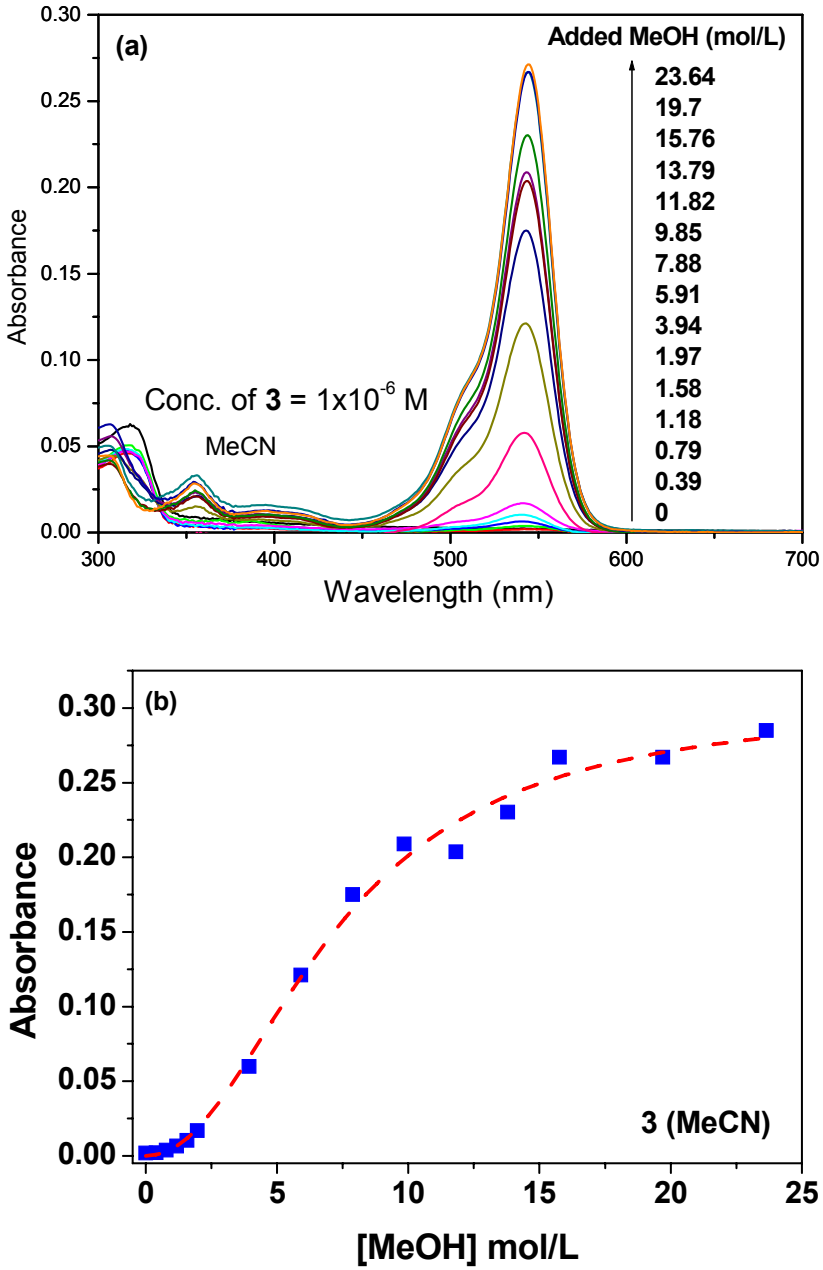

Figure S25. (a) absorption spectra and (b) plot of absorbance of **3** as a function of added MeOH [mol/L] in MeCN (conc. 1×10^{-6} M).

Theoretical Calculations to evaluate primary PET process:

The structure of a fluorophoric system provides vital information towards the thermodynamics of the feasibility of the operative processes. A slight structural modification of the system can perturb its photophysical property significantly. In order to complement the structural aspect of the molecules, geometrical optimization for the fluorophoric system 1 and its fragments were carried out by employing the semi-empirical PM3 method (convergence gradient <0.001, Hyperchem version 7.0, Hypercube Inc).

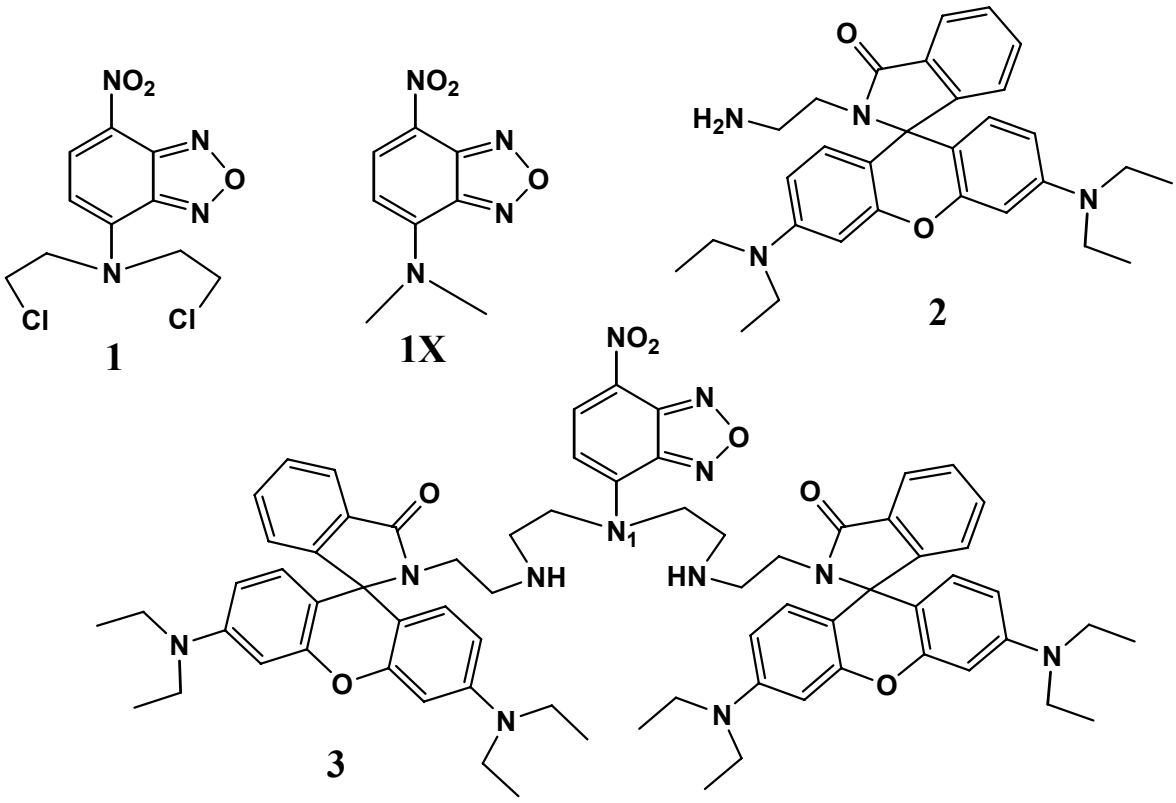

Table S3. Selected geometrical parameters[a] for the systems (**1-3**).

	μ_{TOTAL} (D)	E_{HOMO} (eV)	E_{LUMO} (eV)	$\Delta E_{HOMO-LUMO}$ (eV)	$R_{D-A(NO2)}$ (Å)	$R_{D-A(Rhod-O)}$ (Å)
1	6.21	-9.403	-2.084	7.319	5.836(3)	-
1X	7.83	-9.170	-1.944	7.226	5.832(1)	-
2	6.73	-8.490	-0.384	8.116	-	5.471(0)
3	5.10	-8.872	-1.488	7.384	5.826(7)	3.860(1)

[a] R = distance between donor and acceptor

Figure S26. Electron density map of HOMO and LUMO of the geometrically optimized compounds (**1-3**)

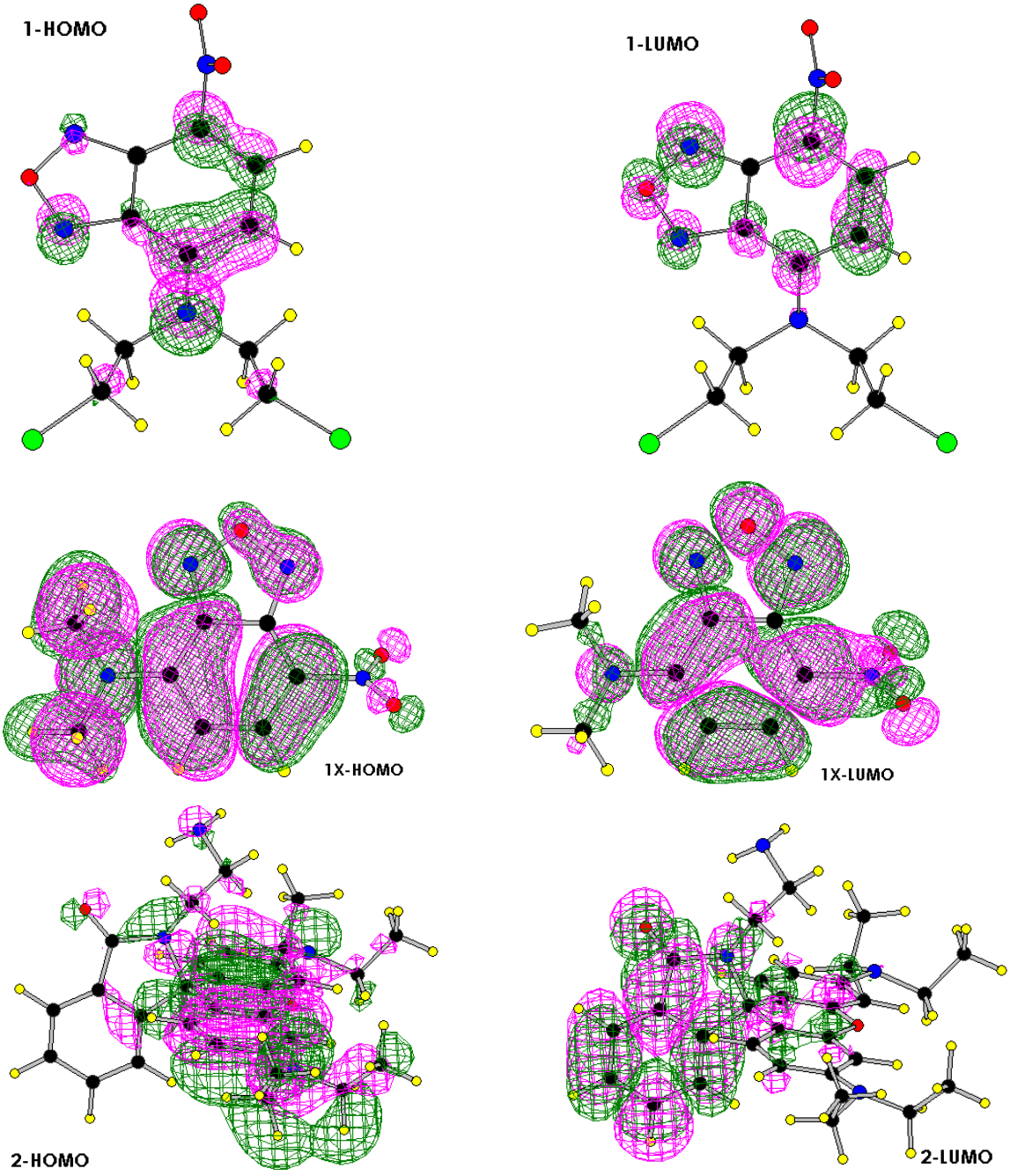

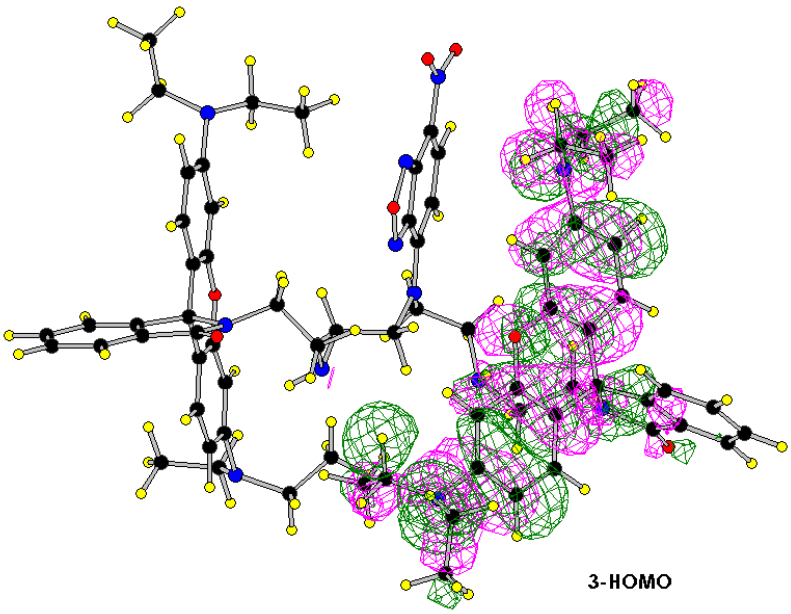

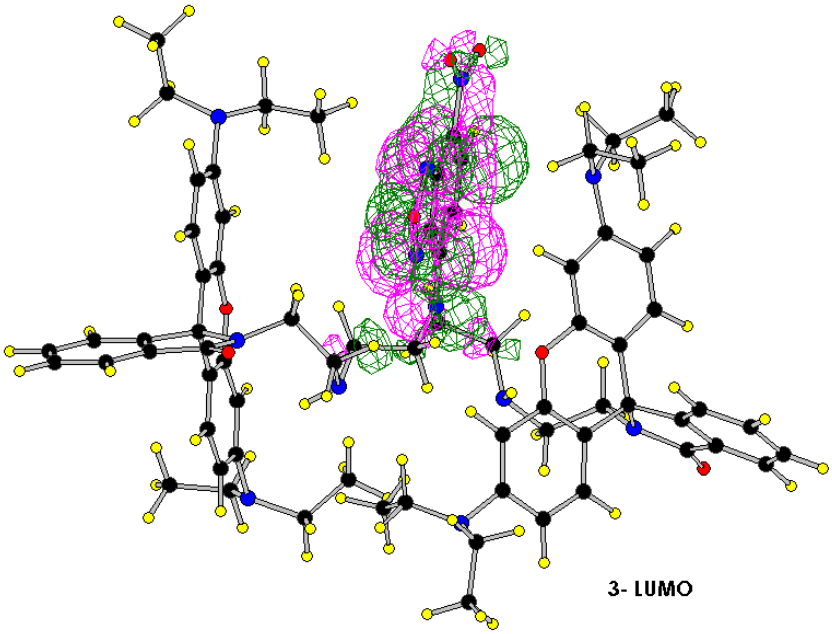

There are various proto-physical processes are operative simultaneously. The Photoinduced electron transfer process can occur from the donor amino N-atom to either the (a) nitro acceptor group of benzofurazan or (b) π-acceptor of the Rhodamine. The feasibility and the effectiveness of PET processes can be evaluated from the theoretical calculations. The electron density map and $\Delta E_{HOMO\text{-}LUMO}$(eV) provide the vital information here as the $\Delta E_{HOMO\text{-}LUMO}$(eV) of the **1** was found to be approximately equal to that of **1X**.

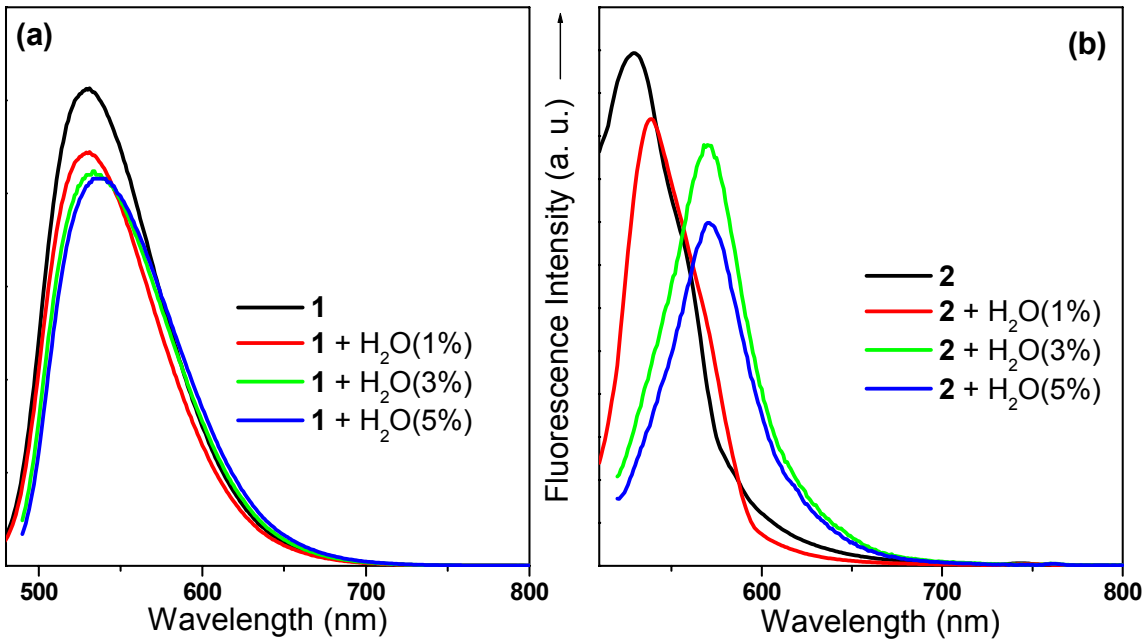

Figure S27. Emission spectra of (a) **1** and (b) **2** in presence of H_2O in MeCN. Concentration of the ligands = 1×10^{-6} M, added water in % of v/v with MeCN given in the parenthesis.

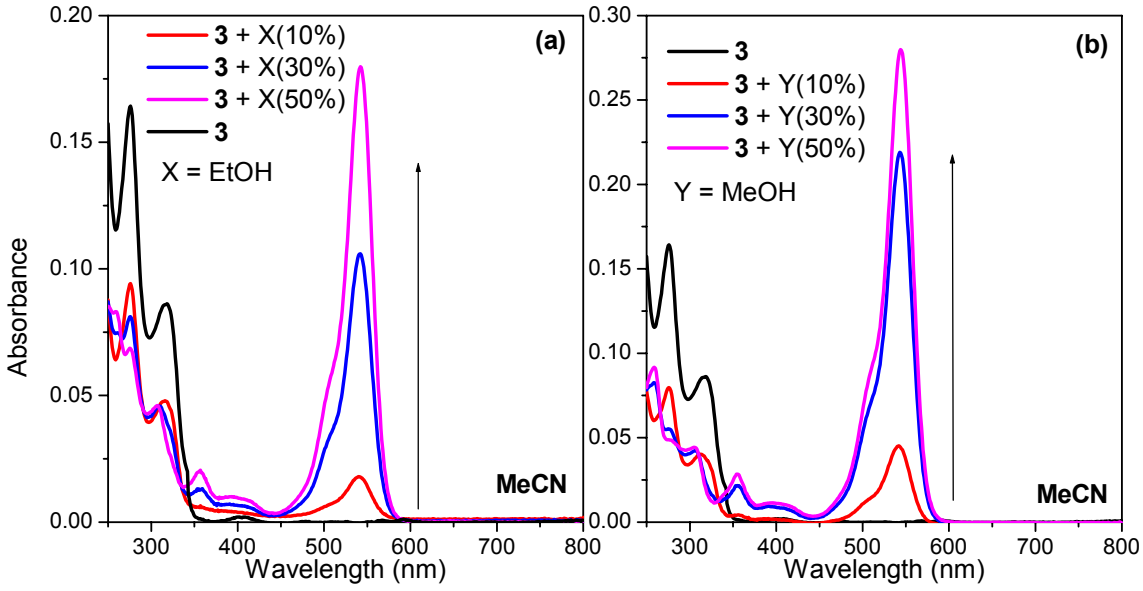

Figure S28. Absorption spectra of **3** in presence of (a) Ethanol and (b) MeOH in MeCN. [conc. = 1×10^{-6} M].

Figure S29. Photographs of **3** alone (a) and in presence of (b) MeOH (10 % v/v), (c) MeOH (30% v/v), (d) MeOH (50 % v/v), (e) EtOH (10 % v/v), (f) EtOH (30 % v/v) and (g) EtOH (50 % v/v) in MeCN [conc. 1×10^{-6} M].

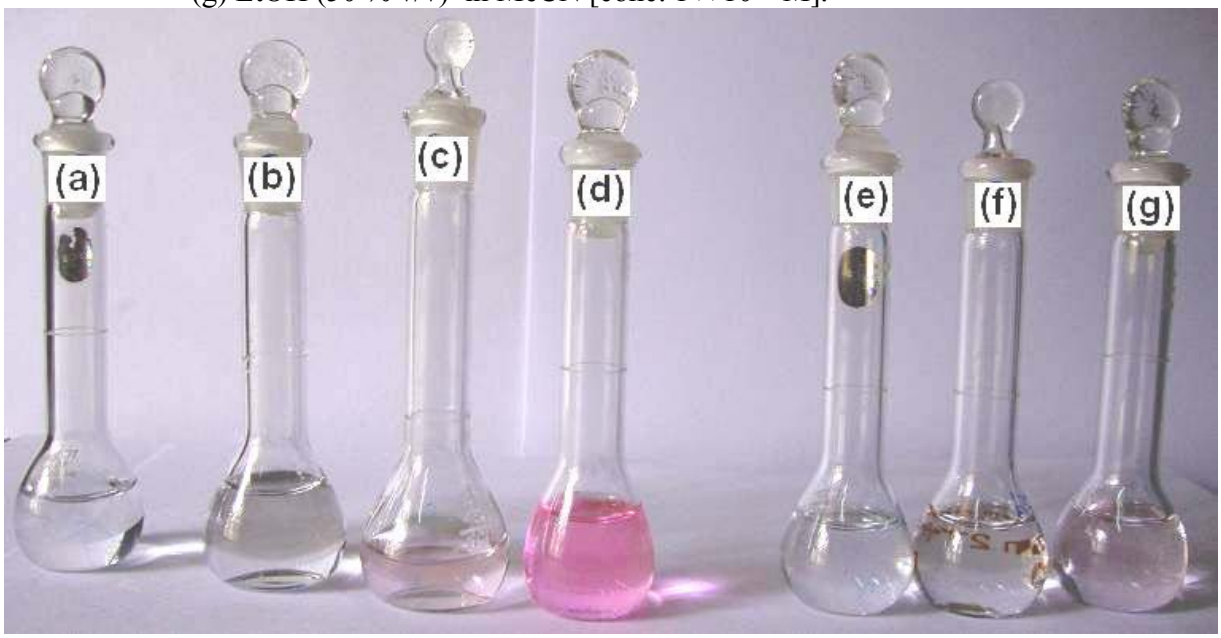

Figure S30. Photographs of **3** alone (a) and in presence of (b) MeOH (10 % v/v), (c) MeOH (30% v/v), (d) MeOH (50 % v/v), (e) EtOH (10 % v/v), (f) EtOH (30 % v/v) and (g) EtOH (50 % v/v) in THF [conc. 1×10^{-6} M].

The absorption spectral(Fig. S15, S25, and S28) pattern and corresponding photographs(Fig. S29, S30) of the micromolar solution of **3** reveals that few protic solvents such as methanol and ethanol also induce spiro-ring opening of **3** as seen in case with H_2O. The comparative absorption spectral pattern reveal that even a small amount of H_2O (3-5 % v/v) results in higher absorption and colour than 50 % v/v of those protic solvents. This infers to a water induced ring opening of spirolactam of **3** with a concentration threshold 3-5 % v/v in organic solvents such as MeCN and THF, where as solvent assisted ring-opening of the spiro-structure occurs as a function of solvent polarity in the case of protic solvents (MeOH and EtOH) in mixed solvents media. The emission spectral pattern follow similar trend as that of the absorption spectra.

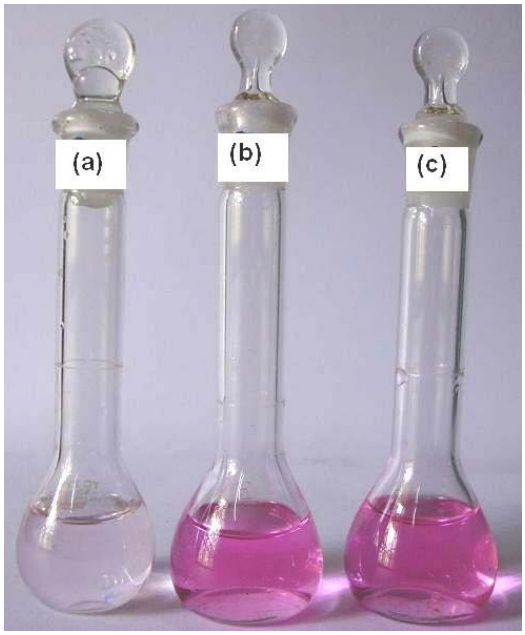

Figure S31. Photographs of **3** in (a) pH 4.0 (b) 7.0 and (c) pH 9.2 [conc. = 1×10^{-6} M].

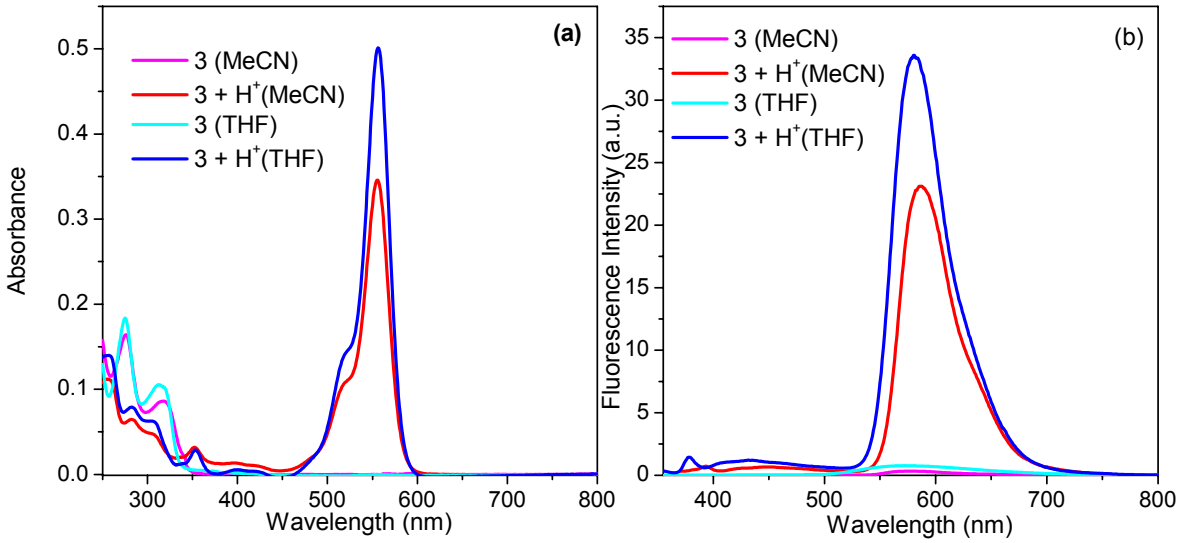

Figure S32. (a) Absorption and (b) emission spectra of **3** alone and in presence of H^+ (TFA) in different solvents, conc. = 1×10^{-6} M. (The fluorescence intensity has been scaled down by a factor 10^6 for clarity).

Figure S33. Photographs of **3** alone in (a) MeCN, (c) THF and in presence of H^+ in MeCN (b) and in THF (d) [conc. 1×10^{-6} M].